Ground-state properties of ferromagnetic metal/conjugated polymer interfaces

S. J. Xie,[1,2] K. H. Ahn,[1] D. L. Smith,[1] A. R. Bishop,[1] and A. Saxena[1]
[1]*Theoretical Division, Los Alamos National Laboratory, Los Alamos, New Mexico 87545*
[2]*School of Physics and Microelectronics, Shandong University, Jinan 250100, People's Republic of China*
(Received 4 September 2002; revised manuscript received 14 November 2002; published 11 March 2003)

We theoretically investigate the ground-state properties of ferromagnetic metal/conjugated polymer interfaces. The work was partially motivated by recent experiments in which injection of spin-polarized electrons from ferromagnetic contacts into thin films of conjugated polymers was reported. We use a one-dimensional nondegenerate Su-Schrieffer-Heeger Hamiltonian to describe the conjugated polymer and one-dimensional tight-binding models to describe the ferromagnetic metal. We consider both a model for a conventional ferromagnetic metal, in which there are no explicit structural degrees of freedom, and a model for a half-metallic ferromagnetic colossal magnetoresistance (CMR) manganite that has explicit structural degrees of freedom. We investigate electron charge and spin transfer from the ferromagnetic metal to the organic polymer, and structural relaxation near the interface. We find that there can be spin density polarization in the polymer near the interface. The spin-density oscillates and decays into the polymer with a decay length of about six times the lattice constant of the polymer. We find an expansion of the end bonds of the CMR manganite segment and a contraction of the polymer bonds near the interface. By adjusting the relative chemical potential of the contact and the polymer, electrons can be transferred into the polymer from the magnetic layer through the interfacial coupling. We calculate the density of states (DOS) before and after coupling for cases in which electrons are transferred and are not transferred to the polymer. The DOS has important consequences for spin injection under electrical bias: polarized spin injection is possible when the Fermi level of the ferromagnet lies below the the bipolaron level of the polymer. However, if the Fermi level of the CMR manganite lies above the bipolaron level of the polymer, the transferred electrons form bipolarons, which have no spin, and there is no spin density in the bulk of the polymer.

DOI: 10.1103/PhysRevB.67.125202 PACS number(s): 72.25.−b, 73.61.Ph, 75.47.Gk, 71.38.−k

I. INTRODUCTION

Magnetoelectronics or spintronics is a field of growing interest. Since the discovery of giant magnetoresistance,[1] rapid progress has been made in this field. Electron spin injection and spin-dependent transport are essential aspects of spintronics and have been extensively studied in a number of different contexts, including: ferromagnetic metals to superconductors,[2] ferromagnetic metals to normal metals,[3] ferromagnetic metals to nonmagnetic semiconductors,[4] and magnetic semiconductors to nonmagnetic semiconductors.[5] Recently, spin-polarized injection and spin-polarized transport in conjugated polymers have been reported.[6] Specifically, spin injection was reported into thin films of the conjugated organic material sexithienyl from half-metallic colossal magnetoresistance (CMR) manganites (in which electron spins at the Fermi surface are completely polarized) at room temperature. The ease of fabrication and low-temperature processing of conjugated organic materials open many possibilities for application, and electronic as well as optoelectronic devices fabricated from these materials (e.g., organic light-emitting diodes and spin valves) are being actively pursued.[6]

Theoretical study of spin-polarized injection and transport has been carried out primarily in the framework of classical transport equations.[7–9] The role of interface properties for spin injection in inorganic semiconductors was investigated in this context.[10–13] The purpose of this paper is to study the ground-state characteristics such as lattice displacements and charge-density and spin-density distribution of conjugated organic polymers contacted with a ferromagnetic metal. An added motivation to study this type of ''active'' interface is that because of relatively large electron-phonon coupling, the materials on *both* sides of the interface can deform, which may facilitate spin-polarized injection. Specifically, we find that both the polymer and the ferromagnetic CMR manganite deform near the interface, thereby altering the charge and spin distribution in the vicinity of the interface.

The paper is organized as follows. In the following section we present tight-binding models for a nondegenerate conjugated polymer, a ferromagnetic (FM) metal, a half-metallic CMR manganite, and the interface between the polymer and the two kinds of magnetic materials. Section III presents the results for a model junction between the polymer and the FM metal, and Sec. IV describes results for CMR manganite/polymer junctions. Our main findings are summarized in Sec. V.

II. MODEL

Organic polymers currently used for electronic and optoelectronic devices typically have a nondegenerate ground state. The first experimental evidence of spin-polarized electrical injection and transport in conjugated organic materials was carried out using sexithienyl (T_6), a π-conjugated oligomer.[6,14] The underlying physics of spin injection and transport is of particular interest for conjugated organic materials, where strong electron-phonon coupling leads to polaronic (or bipolaronic) charged states.[15] These polymers or oligomers have chain structures that can be described using a

nondegenerate version of the one-dimensional Su-Schrieffer-Heeger model, the Brazovskii-Kirova (BK) model,[16,17]

$$H_P = -\sum_{i,\sigma} \epsilon_P a^+_{i,\sigma} a_{i,\sigma} - \sum_{i,\sigma} [t_P - t_1(-1)^i - \alpha_P(u_{i+1} - u_i)] \times (a^+_{i,\sigma} a_{i+1,\sigma} + a^+_{i+1,\sigma} a_{i,\sigma}) + \sum_i \frac{1}{2} K_P (u_{i+1} - u_i)^2. \quad (1)$$

Here $a^+_{i,\sigma}$ ($a_{i,\sigma}$) denotes the electron creation (annihilation) operator at site i with spin σ, ϵ_P is the on-site electron energy of an atom, t_P is the transfer integral in a uniform (undimerized) lattice, α_P the electron-phonon interaction parameter, t_1 introduces nondegeneracy into the polymer, u_i is the lattice displacement at site i, and K_P denotes a spring constant.

To describe a conventional ferromagnetic metal, we use a one-dimensional tight-binding model with kinetic energy H_{ke} and spin splitting H_{Hund} terms:

$$H_{FM} = H_{ke} + H_{Hund}, \quad (2)$$

$$H_{ke} = -\sum_{i,\sigma} t_F (a^+_{i,\sigma} a_{i+1,\sigma} + a^+_{i+1,\sigma} a_{i,\sigma}), \quad (3)$$

$$H_{Hund} = -\sum_i J_i (a^+_{i,\uparrow} a_{i,\uparrow} - a^+_{i,\downarrow} a_{i,\downarrow}), \quad (4)$$

where t_F is the transfer integral for a ferromagnetic metal and H_{Hund} describes the spin splitting of the magnetic atom with site-dependent strength J_i. We take an occupation of one electron per atom and $J_i = J_M$ with parameters $t_F = 0.622$ eV and $J_M = 0.625$ eV for the conventional ferromagnetic metal.

CMR manganites can form half-metallic ferromagnets and are very interesting materials as spin-polarized electron injecting contacts. CMR manganites have a chemical composition such as $Re_{1-x}Ak_xMnO_3$, where Re represents a rare earth atom, e.g., La and Nd, and Ak represents an alkaline-earth metal such as Ca, Sr, and Ba. In these materials, Mn has a valence of $(3+x)$, which depends on the doping concentration x. Depending on doping, the material can be either a metal or an insulator, and either ferromagnetic or antiferromagnetic.[18] In particular, $Re_{1-x}Ak_xMnO_3$ can be a half-metallic ferromagnet when $0.2 < x < 0.5$, for example, with Re=La and Ak=Ca. In this state, all the electrons at the Fermi surface have the same spin orientation. The isolated Mn atom has five electrons in its $3d$ orbitals. These electrons have a parallel spin alignment due to a strong Hund's rule splitting. Because of crystal-field splitting in a solid, three of the orbitals form the low-energy t_{2g} states (of the symmetry form xy, yz, and zx), and the other two form the higher-energy e_g states (of the symmetry form $x^2 - y^2$ and $3z^2 - r^2$). In the ground state, the electrons in t_{2g} are localized and constitute core spins. The e_g states are extended and the electrons in these states can be delocalized. In cubic symmetry, the two e_g levels are degenerate. However, in lower symmetry tetragonal or orthorhombic structures, the degeneracy of the e_g states is broken. In CMR manganites, a structural transition due to a Jahn-Teller coupling causes movement of oxygen ions with respect to the manganese ions, which reduces the symmetry on the Mn ions and breaks the e_g-state degeneracy.

Here, we consider a polymer or an oligomer chain connected at the ends of a CMR manganite lattice in the z direction. We establish a one-dimensional model which contains the basic properties of a half-metallic CMR manganite; a ferromagnetic metal with electron-lattice coupling. The following one-dimensional model captures these essential features:

$$H_{CMR} = H_{ke} + H_{Hund} + H_{el-lat} + H_{elastic}, \quad (5)$$

where H_{ke} and H_{Hund} are given in Eqs. (3) and (4), and

$$H_{el\text{-}lat} = -\sum_{i,\sigma} \lambda_F (u_{i+1} - u_i) a^+_{i,\sigma} a_{i,\sigma}, \quad (6)$$

$$H_{elastic} = \sum_i \frac{1}{2} K_F [(\delta_i - u_i)^2 + (u_{i+1} - \delta_i)^2]. \quad (7)$$

Here u_i and δ_i are the displacements of the ith oxygen atom and manganese atom, respectively. H_{ke} describes electron hopping between two nearest manganese atoms. H_{Hund} describes the spin splitting of a magnetic manganese atom, which results from interaction with the core spins. We have $J_i = J_M$ for the ferromagnetic state (core spins aligned), and $J_i = (-1)^i J_M$ for the antiferromagnetic state. $H_{el\text{-}lat}$ gives the on-site energy of the manganese atoms, which depends on the displacement of the nearest-neighbor oxygen atoms, and λ_F denotes the electron-lattice coupling strength. The last term $H_{elastic}$ represents the elastic energy and includes nearest-neighbor interactions.

There are two main differences between the conventional ferromagnetic metal and the ferromagnetic CMR manganite. One is due to the presence of electron-phonon coupling in the latter case, as is evident from Eqs. (2) and (5). The second difference arises from a combination of the spin splitting Hund's rule term and the electron-phonon interaction in the CMR manganites, which can, for specific alloy compositions, result in the material being half-metallic. Thus, all electrons on the Fermi surface of the CMR manganite can have the same spin orientation. It is clear that both the electron-phonon coupling and this electronic contribution affect the difference in the qualitative behavior in the two cases.

Coupling at the interface between the conjugated polymer and the ferromagnetic metal is described by the hopping integral

$$t_{F\text{-}P} = \beta (t_F + t_P)/2, \quad (8)$$

where β is a weighting parameter. In principle, this coupling could be spin dependent, but here we take $t^{\uparrow}_{F\text{-}P} = t^{\downarrow}_{F\text{-}P} = t_{F\text{-}P}$ for simplicity. Periodic boundary conditions are adopted.

The parameters used for the CMR manganite $Re_{1-x}Ak_xMnO_3$ are $t_F = 0.622$ eV, $J_M = 1.25$ eV, $K_F = 7.4$ eV/Å^2 (Ref. 19), and $\lambda_F = 2.0$ eV/Å. For the organic polymer, we take representative parameters as $t_P = 2.5$ eV,

$\alpha_P = 4.2$ eV/Å, $K_P = 21.0$ eV/Å^2.[20] We set the degeneracy breaking parameter $t_1 = 0.04$ eV so that the energy difference per carbon atom between the two dimerized phases is 0.035 eV. The relative chemical potential ϵ_P was used to adjust the electron transfer between the ferromagnet and the polymer. Segment lengths were taken so that $Re_{1-x}Ak_xMnO_3$ consists of 100 MnO units and the polymer of 100 CH units, that is, $N_M = N_P = 100$. For most of the properties, the results do not depend on the lengths of the segments if they are not too short. The interfacial coupling parameter was taken as $\beta = 1$. If $\beta > 1$, the interface acts as a potential well and tends to confine electrons, whereas if $\beta < 1$ the interface acts as a potential barrier and tends to exclude electrons.

We first study an isolated $Re_{1-x}Ak_xMnO_3$ chain to test the effectiveness of this model for the CMR manganite. The electronic eigenstates

$$|\psi_{\mu\sigma}\rangle = \sum_i Z_{i,\mu,\sigma} a^+_{i,\sigma} |0\rangle \tag{9}$$

corresponding to the eigenvalue $\varepsilon_{\mu,\sigma}$ are solved from the equation

$$-t_F Z_{i+1,\mu,\sigma} - t_F Z_{i-1,\mu,\sigma} - J_i \sigma Z_{i,\mu,\sigma} - \lambda_F (u_{i+1} - u_i) Z_{i,\mu,\sigma} = \varepsilon_{\mu,\sigma} Z_{i,\mu,\sigma}, \tag{10}$$

where $\sigma = +1$ for spin up and -1 for spin down. The displacements $\{\delta_i\}$ and $\{u_i\}$ in the ground state are determined from the eigenstates self-consistently:

$$\delta_i = \frac{1}{2}(u_i + u_{i+1}), \tag{11}$$

$$u_i = \frac{1}{2}\left[\delta_{i-1} + \delta_i - \frac{\lambda_F}{K_F} \sum_{\mu,\sigma} (Z_{i,\mu,\sigma} Z_{i,\mu,\sigma} - Z_{i-1,\mu,\sigma} Z_{i-1,\mu,\sigma}) \right]. \tag{12}$$

If $\lambda_F = 0$, the stable configuration has a uniform structure, i.e., $\delta_i = 0$ and $u_i = 0$, without distortion. Otherwise, some distortion will occur. From Eqs. (11) and (12) we see that the displacements of both oxygen and manganese atoms depend on the electronic density at the manganese atoms.

The structure and magnetism of $Re_{1-x}Ak_xMnO_3$ depend on the doping concentration x that determines the electron number per manganese atom. The orbitals of each manganese atom have been renormalized to a single orbital in the present model, and the electron number per manganese atom is denoted by y ($\leqslant 1$). Figure 1(a) shows the dependence of the energy difference per site between the FM and antiferromagnetic (AFM) states on y. For an electronic doping concentration $y = 0$ (no electrons), the FM and AFM states have the same energy, and the equilibrium conditions give $\delta_i = u_i = 0$. For $y = 1$ (that is, each manganese atom having one electron), the AFM state is lower in energy than the FM state. An energy gap of 2.5 eV appears in the AFM state for both the spin up and down energy levels. The lower subband levels are occupied and the system is an insulator. At $y = 0.5$, the FM state is lower in energy than the AFM state. At this electron concentration, the energy difference between

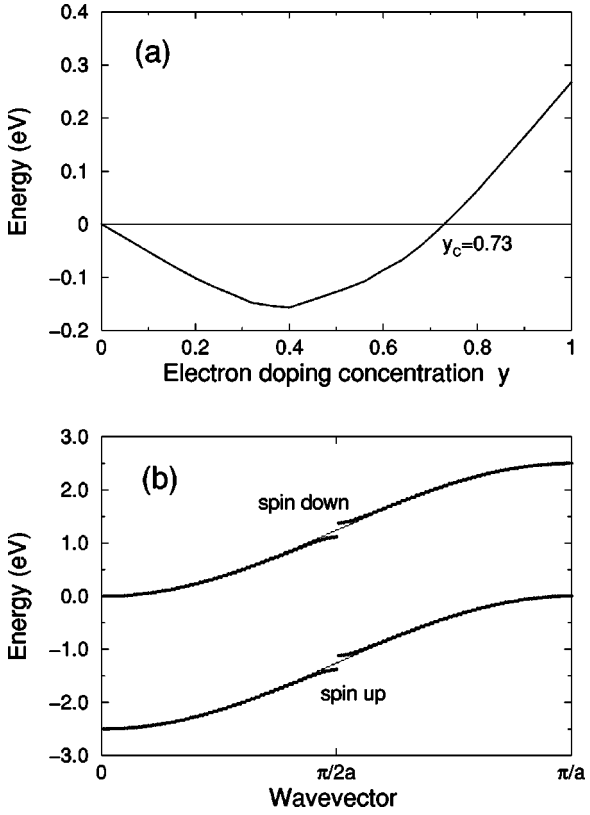

FIG. 1. (a) Dependence of energy difference per site between a one-dimensional ferromagnetic chain and an antiferromagnetic $Re_{1-x}Ak_xMnO$ chain with doping concentration y. (b) Energy levels of $Re_{1-x}Ak_xMnO$ in the ferromagnetic state: $y = 0.5$ (thick line) and $y = 0.32$ (thin line). The upper curve in panel (b) is for spin-down electrons and the lower curve is for spin-up electrons. A gap of 0.26 eV appears at $k = \pi/2a$ in the case of half doping ($y = 0.5$).

FM and AFM states is 0.127 eV per manganese atom. In this case, as shown in Fig. 1(b), the energy bands of the FM state are totally spin split. There is a gap of 0.26 eV at the wave vector $k = \pi/2a$ (a is the lattice constant between two nearest Mn sites), and the system is an insulator. This gap can be adjusted by changing λ_F. When $\lambda_F \leqslant 1.4$ eV/Å, the gap is close to zero. All the spin-down levels are empty, and only the lower sublevels of the spin-up band are occupied. At $y = 0.5$, the charge density has an oscillatory distribution. For example, at $\lambda_F = 2.0$ eV/Å, the densities on two adjacent manganese atoms are about $0.621e$ and $0.379e$ (at $y = 0.5$). Away from $y = 0.5$, the energy gap disappears and the system becomes a ferromagnetic half-metal. In the ferromagnetic state, the sites displace in the approximate pattern,

$$\delta_i = \delta_0 \sin[2i(y - 0.5)\pi], \tag{13}$$

$$u_i = u_0 \cos[2i(y - 0.5)\pi]. \tag{14}$$

With electron concentration $0.2 \leqslant y \leqslant 0.45$, the displacements of both Mn and O atoms become very small ($\delta_0 \leqslant 0.005$ Å and $u_0 \leqslant 0.01$ Å), and decrease to zero when the chain length becomes arbitrarily long. That is, the system becomes uniform in this doping region, and correspondingly, the charge

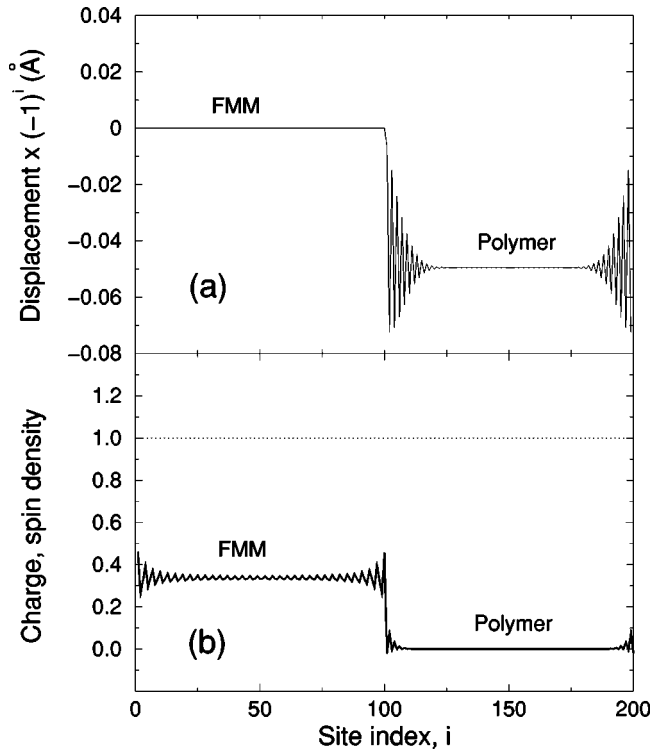

FIG. 2. For a simple ferromagnetic metal (FMM)/polymer chain, (a) site displacements, (b) charge (dotted line) and spin (solid line) density distributions are shown. There is no electron transfer between the FMM and the polymer. The interface is between sites 100 and 101, and $\epsilon_P = 0$. All the site displacements are plotted after multiplying with a factor $(-1)^i$, where i is the site index.

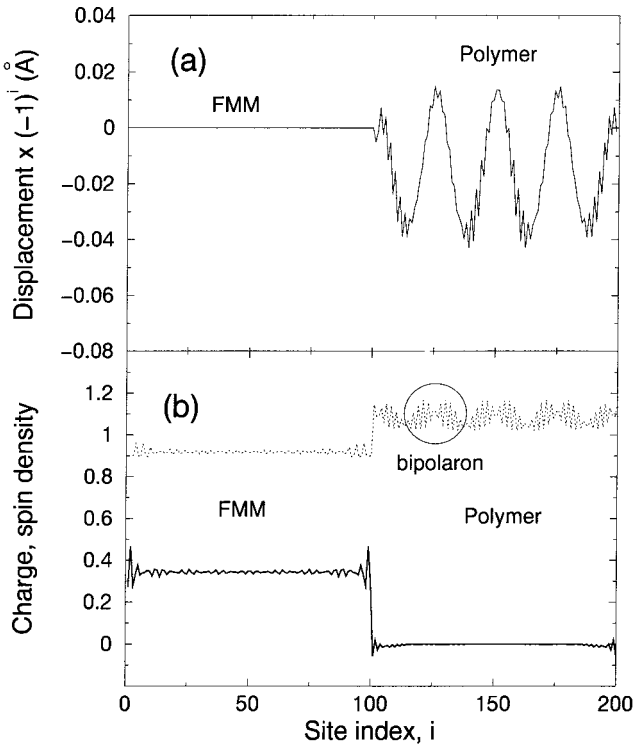

FIG. 3. Same as in Fig. 2, but for $\epsilon_P = 1.0$ eV. Electrons are transferred from the FMM to the polymer through the interface by increasing the chemical potential of the FMM, resulting in bipolarons forming in the polymer.

density is also uniform with a half-metallic property. These results are consistent with the basic properties of the CMR manganites[18] and show that the one-dimensional model gives a reasonable description of them.

III. FERROMAGNETIC METAL/POLYMER JUNCTION

We first consider a polymer chain contacted by a conventional rigid ferromagnetic metal. In the case of half filling and for the parameters used, the spin polarization for the ferromagnet is $\rho = (N_\uparrow - N_\downarrow)/(N_\uparrow + N_\downarrow) = 0.34$. The polymer has a one-dimensional chain structure with a strong electron-lattice interaction that will cause localized charged excitations. When the polymer is connected with a ferromagnetic metal, both the lattice configuration and charge distribution of the polymer are affected. By adjusting the relative chemical potential, electrons (or holes) are transferred into the polymer and cause the displacement of the lattice sites. Results are shown in Figs. 2 and 3 for $\epsilon_P = 0$ and $\epsilon_P = 1.0$ eV, respectively. Following the usual convention, the displacement is plotted with a multiplying factor $(-1)^i$, where i is the site index. The ferromagnetic metal is to the left and the polymer is to the right of the interface, which is between sites $n = 100$ and 101. In Fig. 2, there is no electron transfer between the segments, and the charge density is uniform within the whole system. But the charges near the interface can be spin polarized. The polarization oscillates and decays into the polymer segment. The decay length of the spin polarization is about $6b$, where b is the lattice constant in the polymer. If the chemical potential of the ferromagnet is higher than the bipolaron level in the polymer, as in Fig. 3, electrons are transferred into the polymer segment and reach a new equilibrium for the system. Instead of forming extended electronic waves, the extra electrons in the polymer form localized charged bipolarons. Figure 3(a) shows the displacements of lattice sites, from which we see that, in this case, three complete bipolarons are formed within the polymer together with some local distortions at the interface. The corresponding charge and spin distributions are shown in Fig. 3(b). In the present BK model for the nondegenerate polymer,[16,17] bipolarons are energetically lower than polarons. Since each bipolaron has two confined electronic charges with opposite spins, a bipolaron has no spin. There is neither localized nor extended spin distribution within the polymer layer. Because the polymer is nonmagnetic in the ground state, or more generally at thermal equilibrium, there is no spin distribution far from the interface.

IV. FERROMAGNETIC CMR MANGANITE/POLYMER JUNCTION

Here, we consider the polymer chain in contact with a half-metallic ferromagnetic $Re_{1-x}Ak_xMnO_3$ chain with electron concentration $y = 0.32$. By adjusting the relative chemical potential, electrons are transferred between the CMR manganite and polymer. At $\epsilon_P = 2.15$ eV, there is essentially

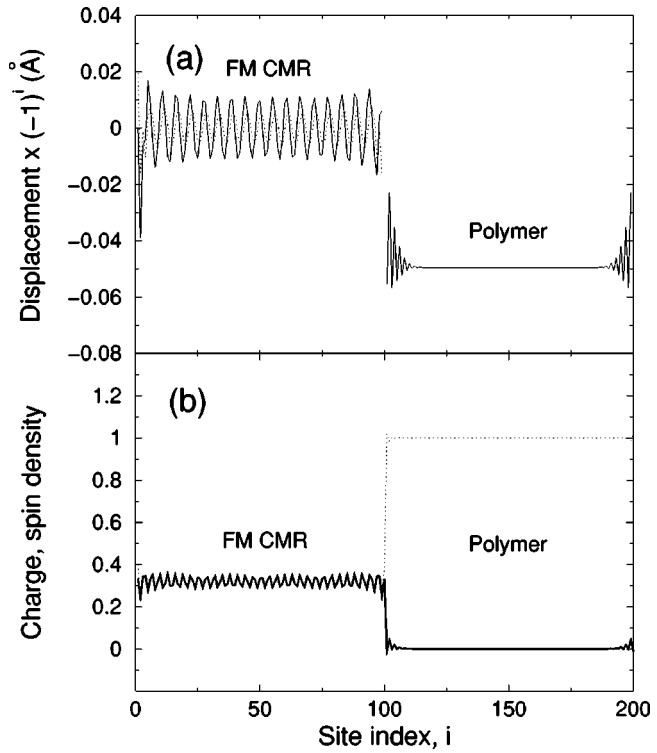

FIG. 4. For a ferromagnetic $Re_{1-x}Ak_xMnO$ (FM CMR manganite)/polymer chain, (a) site displacements of Mn (left dotted), O (left solid), and C (right solid) atoms, and (b) charge (dotted line) and spin (solid line) density distributions are shown. The charge and spin densities coincide in the CMR manganite. There is no electron transfer between the FMM and the polymer. The interface is between sites 100 and 101.

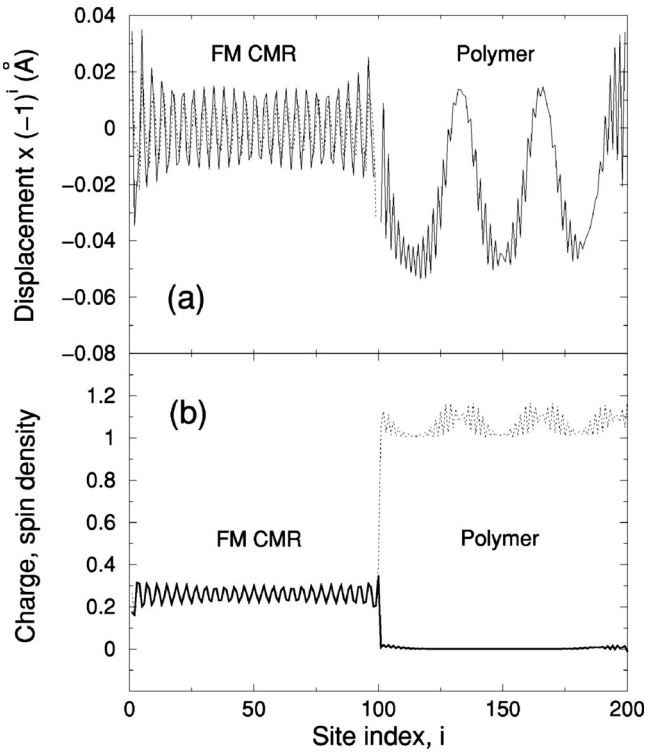

FIG. 5. Same as in Fig. 4 but with some electrons transferred from the FM CMR manganite segment to the polymer through the interface by increasing the chemical potential of the FM CMR manganite, resulting in bipolarons forming in the polymer.

no electron transfer between the segments. Figure 4(a) shows the displacements of the atoms (Mn, O, and C) compared to their uniform bulk positions. Within the CMR manganite segment, both the manganese and oxygen atoms are only slightly displaced. The small displacements are due to the finite length of the segment and disappear as the segment length is increased. The carbon atoms have a displacement of 0.05 Å, corresponding to the bulk dimerization of the polymer chain. The interfacial atoms have a deviation from the bulk dimerization, which results in a small expansion of the end bonds of the CMR manganite segment and a contraction of the first few polymer bonds. The charge and spin densities are shown in Fig. 4(b). Because the CMR material is completely spin polarized at the Fermi surface, the charge and spin densities coincide in this segment. The distributions of charge and spin density in each segment are uniform, except for a small modulation near the interface. The modulation in the CMR manganite is a finite-size effect as discussed previously. There is neither a net charge nor spin distribution within the bulk polymer. When we increase the chemical potential of the CMR manganite, electrons are transferred into the polymer. The results for $\epsilon_P = 2.90$ eV are shown in Fig. 5. At this value for the chemical potential, 6.11 electrons transfer to the polymer segment. The CMR manganite segment keeps a nearly uniform lattice structure except for a small deviation at the interface. In the polymer, bipolaron states form, as seen from the displacements shown in Fig. 5(a). The localized electronic density is shown in Fig. 5(b). The transferred electrons form spinless bipolarons, and there is no spin amplitude within the polymer segment.

These results become more apparent if we examine the change in electronic density of states (DOS) defined by the Lorentz line shape formula

$$g_\sigma(\varepsilon) = \sum_\mu \frac{1}{\pi} \frac{\lambda}{(\varepsilon - \varepsilon_{\mu\sigma})^2 + \lambda^2}, \tag{15}$$

where $\varepsilon_{\mu\sigma}$ is a one-electron energy eigenvalue and λ a phenomenological Lorentz linewidth, which we choose as $\lambda = 0.15$ eV. Figure 6(a) shows the DOS for the CMR manganite/polymer chain before coupling of the two segments (that is, for the two separate material segments), and Fig. 6(b) shows the DOS after coupling. The relative chemical potential was adjusted to be $\epsilon_P = 2.15$ eV as in Fig. 4, so that there is no electron transfer between the CMR manganite and polymer after coupling. From the figure we see that there is still a large gap for the spin-down states, but the gap for spin-up states decreases after coupling. All the occupied states near the Fermi level have spins up, and these states are confined in the segment of the CMR manganite. Increasing the relative chemical potential $\epsilon_P = 2.90$ eV as in Fig. 5, we plot the DOS before and after coupling in Figs. 7(a) and 7(b), respectively. Because the Fermi level of the CMR manganite is above the bipolaron level of the polymer, electrons transfer to the polymer after coupling. They form double-charged bi-

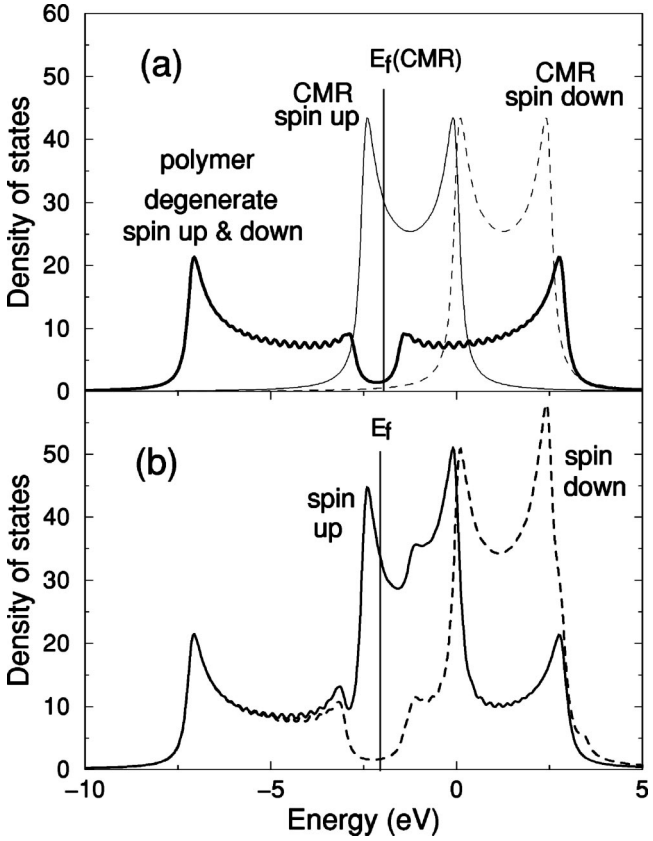

FIG. 6. Density of states of the FM CMR manganite and the polymer, (a) before coupling and (b) after coupling. The thick solid line in (a) is for both spin-up and spin-down electrons in the polymer, the thin solid (dashed) line in (a) is for spin-up (spin down) electrons in the CMR manganite. The solid (dashed) line in (b) is for spin-up (spin down) electrons. The phenomenological Lorentz width is $\lambda = 0.15$. The Fermi level of the CMR manganite lies below the bipolaron energy of the polymer, so that there is no significant electron transfer.

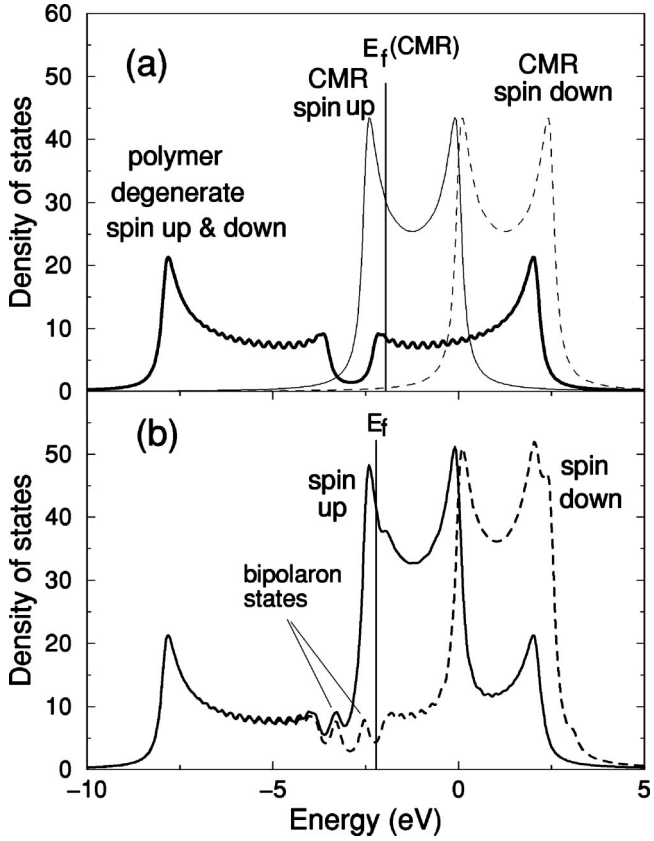

FIG. 7. Same as in Fig. 6, but with the Fermi level of the CMR manganite higher than the bipolaron energy of the polymer, so that electrons transfer from the CMR manganite segment to the polymer after coupling.

polarons. The bipolaron levels are indicated in Fig. 7(b), where the levels of spin-up and -down states overlap. (The spin-up states of the bipolaron near -2.5 eV cannot be seen easily due to the large DOS caused by the CMR manganite.) The difference in DOS of spin up and down at the bipolaron states arises from the effect of the CMR manganite at the interface.

The DOS (in Figs. 6 and 7) has important consequences for spin injection under bias. In Fig. 6, the Fermi level in the CMR manganite lies below the bipolaron level of the polymer and bipolarons are not formed. There is a gap in the spin-down states at the Fermi energy, and the occupied states near the Fermi surface are strongly spin-polarized. Polarized spin injection is possible in this case because a bias voltage will draw spin-polarized electrons from the spin polarized Fermi level of the CMR manganite. By contrast in Fig. 7, the Fermi level in the CMR manganite lies above the bipolaron level of the polymer and a high density of bipolarons is formed in the polymer near the interface. The gap in spin-down states at the Fermi energy is filled because of the bipolaron states. Polarized spin injection is unlikely in this case because a bias voltage will draw electrons from this spin-unpolarized source.

V. CONCLUSIONS

Organic (π-conjugated) polymers differ from traditional inorganic semiconductors due to their strong electron-lattice interactions. Carriers in (nondegenerate) polymers are charged polarons or bipolarons. In this paper we have studied the ground-state properties of a ferromagnetic metal/organic polymer junction. Two kinds of magnetic contacts were considered, a conventional ferromagnetic metal and a CMR manganite ferromagnet with a half-metallic ground state. We presented an effective one-dimensional tight-binding model for both the simple ferromagnetic metal and the half-metallic ferromagnet and explicitly verified that these effective one-dimensional models correctly include the physics of the materials. We found that polarized spin density can occur in the polymer near the interface. The spin density oscillates and decays into the polymer with a decay length of about six times the lattice constant of the polymer. We found an expansion of the end bonds of the CMR manganite segment and a contraction of the polymer bonds near the interface. The calculated density of states indicates that the gap for spin-up states decreases after coupling of polymer and the CMR manganite. The difference in DOS of spin up and

down at the bipolaron states arises from the effect of the CMR manganite at the interface. By adjusting the relative chemical potential, electrons can be transferred into the polymer from the magnetic layer through the interfacial coupling. The DOS has important consequences for spin injection under bias: polarized spin injection is possible when the Fermi level of the CMR manganite lies below the bipolaron level of the polymer. However, if the Fermi level of the CMR manganite lies above the bipolaron level of the polymer, the transferred electrons form bipolarons that have no spin, so that there is no spin density in the bulk of the polymer. Under this condition, the polymer is nonmagnetic, and in the ground state (or more generally at thermal equilibrium), the spin polarization in this material will not be far from the interface.

Static characteristics of the ferromagnetic metal/conjugated polymer interface were investigated in the present model. But major factors have been included, such as lattice relaxation and interfacial coupling. The main motivation for this model came from recent polarized spin injection (and spin-coherent transfer) experiments on the conjugated organic oligomer sexithienyl (thin film) in which a half-metallic ferromagnetic CMR manganite contact was used.[6] This oligomer can serve as an active transport material for potential organic optoelectronic and spintronic devices. Dynamics under external bias will be studied to describe spin injection and polarized spin transport in conjugated organic materials, but an understanding of ground-state properties presented here is required to initiate a study of such dynamics.

ACKNOWLEDGMENTS

This work was supported by the Los Alamos National Laboratory LDRD program.

[1] M.N. Baibich, J.M. Broto, A. Fert, F. Nguyen Van Dau, F. Petroff, P. Etienne, G. Creuzet, A. Friederich, and J. Chazelas, Phys. Rev. Lett. **61**, 2472 (1988).
[2] R. Meservey, Phys. Rev. Lett. **25**, 1270 (1970).
[3] M. Johnson and R.H. Silsbee, Phys. Rev. Lett. **55**, 1790 (1985).
[4] F.G. Monzon, H.X. Tang, and M.L. Roukes, Phys. Rev. Lett. **84**, 5022 (2000).
[5] Y. Ohno, D.K. Young, B. Beschoten, F. Matsukura, H. Ohno, and D.D. Awschalom, Nature (London) **402**, 790 (1999).
[6] V. Dediu, M. Murgia, S. Barbanera, and C. Taliani, in *Electronic Properties of Molecular Nanostructures*, edited by Hans Kuzmany, Jörg Fink, Michael Mehring, and Siegmar Roth, AIP Conf. Proc. No. 591 (AIP, Melville, NY, 2001), p. 548; V. Dediu, M. Murgia, F.C. Matacotta, C. Taliani, and S. Barbanera, Solid State Commun. **122**, 181 (2002).
[7] P.C. van Son, H. van Kempen, and P. Wyder, Phys. Rev. Lett. **58**, 2271 (1987).
[8] G. Schmidt, L.W. Molenkamp, A.T. Filip, and B.J. van Wees, cond-mat/9911014 (unpublished).
[9] I. Zutic, J. Fabian, and S. Das Sarma, Phys. Rev. Lett. **88**, 066603 (2002).
[10] E.I. Rashba, Phys. Rev. B **62**, R16 267 (2000).
[11] D.L. Smith and R.N. Silver, Phys. Rev. B **64**, 045323 (2001).
[12] J.D. Albrecht and D.L. Smith, Phys. Rev. B **66**, 113303 (2002).
[13] G. Schmidt, D. Ferrand, L.W. Molenkamp, A.T. Filip, and B.J. van Wees, Phys. Rev. B **62**, R4790 (2000).
[14] M. Muccini, M. Schneider, and C. Taliani, Synth. Met. **116**, 301 (2001).
[15] K. Waragai, H. Akimichi, S. Hotta, H. Kano, and H. Sakaki, Phys. Rev. B **52**, 1786 (1995).
[16] S.A. Brazovskii and N.N. Kirova, Pis'ma Zh. Éksp. Teor. Fiz. **33**, 6 (1981) [JETP Lett. **6**, 4 (1981)].
[17] S.J. Xie, L.M. Mei, and D.L. Lin, Phys. Rev. B **50**, 13 364 (1994).
[18] See, e.g., S. Jin, T.H. Tiefel, M. McCormack, R.A. Fastnacht, R. Ramesh, and L.H. Chen, Science **264**, 413 (1994); A.J. Millis, Nature (London) **392**, 147 (1998); M.B. Salamon and M. Jaime, Rev. Mod. Phys. **73**, 583 (2001).
[19] K.H. Ahn and A.J. Millis, Phys. Rev. B **61**, 13 545 (2000).
[20] A.J. Heeger, S. Kivelson, J.R. Schrieffer, and W.P. Su, Rev. Mod. Phys. **60**, 781 (1988).